# Efficient numerical solution for highly transient flows

Haroun Mahgerefteh*, Adeyemi O. Oke
Department of Chemical Engineering, University College London,
London WC1E 7JE

Yuri Rykov
Keldysh Institute of Applied Mathematics, Miusskaya sq. 4, 125047, Moscow, Russia

**Abstract**

The numerical solutions for different formulations of the conservation equations based on the dependent variables, pressure ($P$), enthalpy ($h$), density ($\rho$), entropy ($s$) and flow velocity ($u$) for highly transient flows are presented. The models are each in turn applied for simulating the transient fluid flow dynamics following the rupture of a real and a number of hypothetical pipelines containing liquid, flashing liquid, two-phase and a permanent gas. In the case of the flashing liquid and two-phase pipelines, a significant reduction in the computational run time for the *Phu* and *Psu* based simulations as compared to the conventional $P\rho u$ formulation is observed. The above effect is found to be much less pronounced for the for the liquid and permanent gas inventories.

*Keywords:* Process safety, Pipeline rupture, Hazard assessment, Numerical simulation, Computational fluid dynamics, Two-phase flow.

* Author for correspondence (h.mahgerefteh@ucl.ac.uk)

## Introduction

Pressurised pipelines are extensively used for the transport of large quantities of highly flammable hydrocarbons and their rupture can give rise to catastrophic consequences. Indeed in recent years there have been many instances of pipeline rupture (Bond, 2002; Fletcher, 2001) which have caused enormous damage to the environment and numerous fatalities, the most recent example being the Belgium pipeline rupture (Georges and Louvain-la-Neuve, 2005) leading to 25 deaths and 50 injuries. In the United States alone there are over 420,000 km of high pressure gas pipelines, over 250,000 km of oil and products pipelines and many

thousands of kilometres of lower pressure local distribution gas lines. Data published by the U.S. Department of Transport (1997) on reportable incidents reveals that action by third parties alone during 1982 – 1997 caused more than 104,000 incidents of pipeline damage.

The accurate prediction of outflow and its variation with time following pipeline rupture are therefore extremely important since this information dictates all the major consequences associated with such failure including fire, explosion and environmental pollution.

The development of a transient two-phase fluid outflow model for pipeline rupture entails three main steps. The first requires the formulation of the conservation equations governing the flow incorporating heat transfer and frictional effects. The conventional approach has invariably involved expressing these equations in terms of the dependent variables, pressure, density and flow velocity (see for example Picard and Bishnoi 1988,1989; Chen et al., 1992,1993; Mahgerefteh et al., 1999,2000). The resulting quasi-linear partial differential equations are hyperbolic and cannot be solved analytically as they contain terms that are unknown or complex functions of their dependent and independent variables (see Flatt, 1986; Mahgerefteh et al., 1999). The second step involves the transformation of these non-linear equations into a finite difference form. The final step requires their solution in conjunction with the relevant boundary conditions using a suitable numerical technique. As all of these techniques involve the numerical discritisation of the pipeline into a large number of elements, the solution for a typical pipeline often requires very long CPU time (e.g 5 days on a Pentium IV processor for a 300 km, 1 m dia pipeline transporting a condensable hydrocarbon mixture at 100 bar pressure). This is despite significant advances involving the use of nested grid systems (Chen et al., 1992, Mahgerefteh et al., 1999, Oke et al., 2003) and higher speed computer processing powers.

In this study a more fundamental approach is described which for the first time demonstrates the significant effect of the choice of the dependent variables in the formulation of the conservation equations on the computational run time. The model's efficacy is demonstrated based on comparisons with recorded data for the rupture of a real pipeline as well as a number of hypothetical pipelines containing liquid, flashing liquid, two-phase and a permanent gas.

## Theory

### Conservation Equations

The conservation equations are the fundamental building blocks for formulating the transient fluid flow process. The following describes their derivation for 1-D flow in pipes based on different combinations of the primitive parameters including density, entropy and enthalpy. The modelling takes account of heat transfer and friction but assumes homogeneous equilibrium flow with negligible fluid/structure interactions. Comparisons with real data have shown (Chen et al., 1995) that the homogeneous flow assumption in which the constituent phases are at thermal and mechanical equilibrium is valid in the case of rupture of long (>100 m) pipelines. As such only one set of mass, momentum and energy conservation equations suffice for both single and two-phase flows. The pressure waves generated within the contained fluid following rapid depressurisation of a pipeline exert forces that may cause a compliant (freely suspended) system to move or vibrate. This dynamic phenomenon is known as fluid-structure interaction. In this work, such forces are neglected as the pipeline is assumed to be rigidly clamped and inelastic.

### Mass conservation

For an element of fluid, the law of conservation of mass can be expressed as (Versteeg and Malalasekera, 1995):

$$\frac{d\rho}{dt} + \rho\frac{\partial u}{\partial x} = 0 \qquad (1)$$

where $u$ and $\rho$ are the fluid velocity and density with $t$ and $x$, representing time and distance respectively.

For $P = f(\rho, s)$, we have

$$dP = \left(\frac{\partial P}{\partial \rho}\right)_s d\rho + \left(\frac{\partial P}{\partial s}\right)_\rho ds \qquad (2)$$

but

$$\left(\frac{\partial P}{\partial \rho}\right)_s = a^2 \qquad (3)$$

and defining

$$\left(\frac{\partial P}{\partial s}\right)_r = \boldsymbol{j} \tag{4}$$

where $P$, $s$ and $a$ are the fluid absolute pressure, specific entropy and velocity of sound respectively. Substituting equations (3) and (4) into equation (2), the substantial derivative of density with time may be expressed as:

$$\frac{d\boldsymbol{r}}{dt} = \frac{1}{a^2}\left(\frac{dP}{dt} - \boldsymbol{j}\frac{ds}{dt}\right) \tag{5}$$

For any fluid, the total derivative of enthalpy, $h$ is given by (Walas, 1987):

$$dh = Tds + \frac{1}{\boldsymbol{r}}dP \tag{6}$$

or

$$\frac{1}{T}\left[\frac{dh}{dt} - \frac{1}{\boldsymbol{r}}\frac{dP}{dt}\right] = \frac{ds}{dt} \tag{7}$$

Substituting equation (7) into equation (5) and rearranging, the total derivative of density with respect to time in the mass conservation equation (1) may be expressed in terms of fluid pressure and enthalpy for 1D flow as given by:

$$\frac{d\boldsymbol{r}}{dt} = \frac{1}{a^2}\left[\frac{dP}{dt}\left(1 + \frac{\boldsymbol{j}}{\boldsymbol{r}T}\right) - \frac{\boldsymbol{j}}{T}\frac{dh}{dt}\right] \tag{8}$$

Substituting equation (5) into equation (1) produces the mass conservation equation expressed in terms of pressure and entropy for 1D flow:

$$\frac{dP}{dt} - \boldsymbol{j}\frac{ds}{dt} + \boldsymbol{r}a^2\frac{\partial u}{\partial x} = 0 \tag{9}$$

Similarly, substituting equation (8) into equation (1) produces the mass conservation equation expressed in terms of pressure and density for 1D flow:

$$[\,\rho T + \phi\,]\frac{dP}{dt} - \rho\phi\,\frac{dh}{dt} + \rho^2 a^2 T\,\frac{\partial u}{\partial x} = 0 \qquad (10)$$

**Momentum conservation**

In this study, the momentum conservation equation is based on the assumption that only the surface and gravitational body forces are of significance. Furthermore, the bulk of the fluid is assumed to be inviscid, while viscous effect terms that remain appear as external source terms due to wall friction. As such, internal surface force terms due to tangential and normal viscous stresses are ignored. This simplification can be said to be generally acceptable for turbulent flows such as those prevailing during pipeline rupture (see Chen et al., 1995; Mahgerefteh et al., 1999; Picard and Bishnoi, 1988, 1989). Consequently, the momentum equation may be expressed in differential form as (Versteeg and Malalasekera, 1995):

$$\rho\frac{du}{dt} = -\frac{\partial P}{\partial x} - \rho g \sin\theta + \beta_{wx} \qquad (11)$$

where $g$, $\theta$ and $\beta_{wx}$ are the acceleration due to gravity, the angle of elevation and wall frictional force respectively.

**Energy conservation**

Based on the assumptions of inviscid flow, the absence of external work done on, or by the flowing fluid and convective heat transfer being the dominant mode of heat transfer, the energy conservation equation for 1-D flow expressed in terms of pressure and enthalpy is given by (Versteeg and Malalasekera, 1995):

$$\rho\frac{dh}{dt} - \frac{dP}{dt} = q_h - u\beta_{wx} \qquad (12)$$

where $q_h$ is the pipe wall/ambient heat transfer rate.

Multiplying equation (7) by $\rho T$ and substituting the result into equation (12) produces the energy conservation equation expressed in terms of fluid entropy:

$$\tilde{n}T\frac{ds}{dt} = q_h - u\hat{a}_{wx} \qquad (13)$$

Replacing the total derivatives with partial derivatives in space and time, the system of conservation equations (10), (11) and (12) expressed in terms of pressure, enthalpy and velocity (*Phu*) as dependent variables are respectively given by:

$$\left[\, \rho T + \kappa \,\right]\left(P_t + uP_x\right) - \rho\kappa\left(h_t + uh_x\right) + \rho^2 a^2 T\left(u_x\right) = 0 \quad \{\text{mass}\} \tag{14}$$

$$\rho\left(u_t + uu_x\right) + \left(P_x\right) = \alpha \quad \{\text{momentum}\} \tag{15}$$

and

$$\rho\left(h_t + uh_x\right) - \left(P_t + uP_x\right) = \gamma \quad \{\text{energy}\} \tag{16}$$

where:

$$\alpha = -\rho g \sin\theta + \beta_{wx} \tag{17}$$

and

$$\gamma = q_h - u\beta_{wx} \tag{18}$$

Similarly applying the same treatment to equations (9), (11) and (13), the conservation equations expressed in terms of pressure, entropy and velocity (*Psu*) are given by:

$$\left(P_t + uP_x\right) - \kappa\left(s_t + us_x\right) + \rho a^2\left(u_x\right) = 0 \quad \{\text{mass}\} \tag{19}$$

$$\rho\left(u_t + uu_x\right) + \left(P_x\right) = \alpha \quad \{\text{momentum}\} \tag{20}$$

and

$$\rho T\left(s_t + us_x\right) = \gamma \quad \{\text{energy}\} \tag{21}$$

The conservation equations represented by equations (14) - (16) and (19) - (21) are quasilinear. This is because all the derivative terms are linear. Furthermore they are hyperbolic as they can be shown (Prasad and Ravindran, 1985) to possess three real and distinct eigenvalues. These equations cannot be solved analytically as the coefficients of the partial derivatives such as density, $\rho$ or flow velocity, $u$ are themselves functions of some of the dependent functions, $P$, $s$, $h$ and $u$.

**Numerical Solution of the Conservation Equations**

In this work, the Method of Characteristics (MOC) (Zucrow and Hoffman, 1976, Mahgerefteh et al., 1997, 2000) is employed as the numerical solution technique for the resolution of the governing conservation equations. This is due to MOC's superior robustness and accuracy as compared to other numerical techniques such as the finite difference (Chen et al., 1993, Chenet al., 1995, Bendiksen et al., 1991) or finite element methods (Lang, 1991, Bisgaard et al., 1987, Gato and Henriques, 2005).

MOC involves replacing the conservation equations with the corresponding characteristics and compatibility equations and solving them numerically at selected space and time intervals along the pipeline subject to the Courant-Friedrich-Lewy stability criterion (Zucrow and Hoffman, 1976).

**The compatibility equations**

The following describes the main steps for conversion of the partial differential conservation equations derived above into ordinary differential equations, hereby referred to as the compatibility equations.

The two most common methods of deriving the compatibility equations are the matrix transformation method (see Tiley, 1989) and that of multiplying the conservation equations by unknown parameters and subsequent summation (Lister, 1960; Wylie and Streeter 1978; Zucrow and Hoffman, 1976). The latter method is adopted in this study due to its simplicity and mathematical rigour. Its application to the *Phu* equations (14) – (16) results in:

$$(\lambda - u)\left[(\lambda - u)^2 - a^2\right] = 0 \qquad (22)$$

where:

$$\lambda = \frac{dx}{dt} \qquad (23)$$

Equation (22) has three roots. All three turn out to be identical to the path line and mach line characteristics lines derived starting from pressure, density and velocity ($P\rho u$) conservation system of equations (Zucrow and Hoffman, 1976). These are given by

$$\lambda - u = 0$$

$$\lambda_0 = \left(\frac{dx}{dt}\right)_0 = u \qquad \text{(path line)} \qquad (24)$$

The other two roots are obtained as:

$$(\lambda - u)^2 - a^2 = 0$$

$$\lambda - u = \pm a$$

$$\lambda_\pm = \left(\frac{dx}{dt}\right)_\pm = u \pm a \qquad \text{(positive and negative mach lines)} \qquad (25)$$

Following Wylie and Streeter (1978), it can be shown that the *Phu* path line compatibility equation along the path line characteristic curve ($\lambda_0$) is given by:

$$\rho d_0 h - d_0 P = \gamma d_0 t \quad \text{along} \quad \frac{d_0 x}{d_0 t} = u \qquad \{Phu \text{ based}\} \qquad (26)$$

Similarly, the compatibility equations for the positive, $C_+$ and negative, $C_-$ characteristic lines are respectively given by:

$$d_+ P + [\rho a] d_+ u = \left[\frac{j\gamma}{\rho T} + a\alpha\right] d_+ t \quad \text{along} \quad \frac{d_+ x}{d_+ t} = u + a \qquad (27)$$

$$d_- P + [\rho a] d_- u = \left[\frac{j\gamma}{\rho T} - a\alpha\right] d_- t \quad \text{along} \quad \frac{d_- x}{d_- t} = u - a \qquad (28)$$

Following the same methodology, the path line compatibility based on the *Psu* (equations (19) - (21)) and *P*$\rho$*u* (equations (1), (11) and (12)) conservation equations are respectively given by given by:

$$d_0 s = \left[\frac{\gamma}{\rho T}\right] d_0 t \quad \text{along} \quad \frac{d_0 x}{d_0 t} = u \qquad \{Psu \text{ based}\} \qquad (29)$$

$$d_0 P - a^2 d_0 \rho = \frac{j\gamma}{\rho T} d_0 t \quad \text{along} \quad \frac{d_0 x}{d_0 t} = u \qquad \{P\rho u \text{ based}\} \qquad (30)$$

The corresponding compatibility equations for the positive, $C_+$ and negative, $C_-$ characteristic lines based on the *Psu* and *P*$\rho$*u* conservation equations turn out to be exactly the same as

those based on the *Phu* conservation equations (i.e equations (27) and (28) respectively). Hence only the path line compatibility is dependent on the choice of the dependent variables in the formulation of the conservation equations. As such any improvements in CPU times and simulation accuracy based on either of the three different formulations of the conservation equations are entirely dictated by the effectiveness of the corresponding path line compatibility.

The fluid properties at the intersection of the characteristics lines are obtained by expressing the compatibly equations in finite difference form followed by their solution in conjunction with the corresponding characteristics lines using the Euler Predictor-Corrector method (Zucrow and Hoffman, 1976). This involves interpolations coupled with successive improvements in the first order approximations until convergence for a given degree of tolerance is obtained. The above procedure is the main cause of the long CPU times which characterises the use of the MOC, as each iteration step requires the solution of the equation of state.

Expressing the *Phu* compatibility equation (26) in the first order finite difference form, the fluid enthalpy, $h_j$ at the solution point for the predictor step is given by the

$$h_j = \frac{\gamma_0 \Delta t + \left(P_j - P_0\right) + \rho_0 h_0}{\rho_0} \tag{31}$$

Similarly based on the *Psu* compatibly equation (29), the entropy at the solution point is given by:

$$s_j = \left[\frac{\gamma_0}{\rho_0 T_0}\right]\Delta t + s_0 \tag{32}$$

While for the conventionally used *Pru* system of equations (Picard and Bishnoi 1988,1989; Chen et al., 1992,1993; Mahgerefteh et al., 1999,2000), expressing the corresponding compatibility equation (i.e. equation (30)) in the finite difference form produces:

$$\rho_j = \frac{\left(P_j - P_o\right) - \left[\frac{\varphi_o \gamma_o}{\rho_o T_o}\right]\Delta t + a_o^2 \rho_o}{a_o^2} \tag{33}$$

Once the fluid enthalpy or entropy are determined from equations (31) and (32) respectively, the remaining fluid properties (e.g. $\rho$, $\mu$ and $T$) at the solution point may simply be obtained directly from *P/h* and *P/s* flash calculations.

The determination of the fluid properties from the *Pρu* compatibility equation (33) however requires its iterative solution. Presenting the equation in the following form:

$$\rho_j - \rho\left(T_j, P_j\right) = 0 \qquad (34)$$

The solution is a root finding problem where a temperature, $T_j$ is sought such that the density predicted from an isothermal flash calculation using $P_j$ and $T_j$ matches the density, $\rho_j$ obtained from the compatibility equation. The Brent iterative method (Press et al., 1994) is employed for this purpose as it gives rapid convergence (Mahgerefteh et al., 1999). Nonetheless, for two-phase flows, the solution of equation (34) is extremely computationally expensive as numerous isothermal flash calculations are required in order to obtain an accurate solution.

The following investigates the effects of choosing either of the three different forms of the compatibility equations based on the *Phu*, *Psu* and *Pρu* system of conservation equations on the simulation run time and accuracy using the results of Isle of Grain pipeline rupture tests (Richardson and Saville, 1996 a,b) as a case example as well as three other pipelines each containing a permanent gas, liquid and two-phase mixture. The Isle of Grain test results are chosen here since they are the most comprehensive experimentally obtained data available in the open literature.

**Results and Discussion**

The Isle of Grain experiments conducted jointly by BP and Shell (Richardson and Saville, 1996a) involved the rapid depressurisation of an extensively instrumented carbon steel, 154 mm i.d, 100 m pipeline containing commercial propane or LPG (95 % propane, 5% n-butane). Pressure transducers and thermocouples were attached along the line. Inventory and hold-up were measured using load-cells and neutron back scattering.

A number of tests involving both full bore rupture as well as puncture at different starting line pressures were conducted. Of these, the full bore rupture test (P40) initiated by the

rupture of a disc at the downstream end of the pipeline is chosen as an example as it starts with the highest line pressure of 21.6 bara representing the longest discharge duration. The feed and the ambient temperatures are both 20 $^{o}$C. The heat transfer calculations are based on the lumped capacitance method (Myers, 1971), for which respective wall density, specific heat capacity and thermal conductivity of 7854 kg/m$^3$, 434 J/kgK and 53.60 W/mK for carbon steel are assumed (Perry, 1997). The pipeline thickness and roughness factor are given as 0.0073 m and 0.00005 m respectively. The discretisation scheme used for the numerical simulations is based on the specified time intervals using a uniform grid spacing of 2.5 m. Smaller grid sizes were found to have negligible effect on the simulation results.

Figures 1 - 4 respectively show the measured pressure (open and intact end), temperature and inventory variations with time for test P40 in comparison with simulated results using the Pρu, Phu and Psu models.

Referring to figure 1, the transition of the liquid inventory to the 2-phase mixture upon full bore rupture results in an almost instantaneous drop in the rupture plane pressure from 21 bara to ca. 6.5 bar. This is followed by a slower, almost monotonous drop in pressure corresponding to vaporisation of the 2-phase mixture to the gaseous state at around 20s following depressurisation. Similar trends in behaviour may be observed for the variations of the intact end pressure (figure 2) and fluid temperature (figure 3) with time with exception of the effects being less marked. The inventory versus mass data indicates that almost the entire content of the pipeline is discharged in approximately 20s.

Returning to the simulation data, all three models produce good agreement with measured data (curves A) with the *Phu* model (curves C) producing the best fit followed by the *Psu* (curves D) and the *Pρu* (curves B) based predictions. Also, at any given time, the three models predict lower pressures and temperatures when compared to measured data. The *Pρu* model generally predicts the lowest pressures and temperatures at a given time, hence the fastest depressurisation rate, followed by the Psu and Phu models. The *Pρu* model's estimation of the depressurisation time is the most conservative of the three.

The open end pressure-time profile data based on the *Pρu* model (figure 1, curve B) using density as the primitive variable fluctuate between ca 5 - 7.5 bara for the first 1.5 s of depressurisation. This is believed to be due to the rapid change in fluid density during the transition from the liquid to the 2-phase region, which is in turn manifested in instability in

the data. No such marked fluctuations in the results based on the *Psu* and *Phu* models are observed (curves C and D). This is a consequence of the fact that the rates of change in fluid entropy and enthalpy with pressure as the phase transition is crossed are much less pronounced as compared to the variation in the fluid density. This leads to the greater observed stability of the *Phu* and *Psu* based simulation data.

Apart from agreement with field data, the most significant aspect of the simulated data is the associated computation run times. The computation run time for the conventional *Pru* based model is 86 minutes. The corresponding values for the *Phu* and *Psu* models are only 7 and 9 minutes respectively, representing a remarkable 10 fold reduction in the computation run time.

Figures 6 – 8 show simulated discharge rate versus time data following the full bore rupture of relatively long hypothetical pipelines containing various inventories. The corresponding computation run times as well as the pertinent operating conditions are given in the figure legends. Figure 6 represents data for the rupture of a 25 km pipeline containing pure pentane which remains in the liquid state throughout the discharge process. Figure 7 on the other hand refers to a methane (95%) and ethane (5%) mixture pipeline which behaves as a permanent gas during depressurisation. The pipeline length is again 25 km. Finally figure 8 shows the results for a two-phase ethylene (99%) and methane (1%) pipeline. A shorter pipeline length of 5 km was used in this case in view of the significant computation run time.

Returning to figures 6 – 8, the important features in the data may be summarised as follows:

i) All simulations follow the same hyperbolic trend characterised by a marked drop in the discharge rate with time to a steady value soon after depressurisation. In the case of the liquid pipeline (figure 6), the drop in the discharge rate is almost instantaneous. This is consistent with the expected behaviour of a compressed liquid which will instantaneously dissipate its stored energy upon depressurisation.

ii) The observed secondary rapid drop in the discharge rate of the liquid approximately 55s following rupture coincides with the reflection of the depressurisation induced expansion wave from the intact end of the pipeline to the rupture plane.

iii) The discharge rate upon rupture is highest in the case of the liquid (ca. 71000 kg/s; figure 6) followed by two-phase (ca. 16000 kg/s; figure 8) and gas (5500 kg/s; figure 7). This trend is consistent with the initial discharge rate increasing with the fluid density as to be expected.

iv) There are no obvious differences in the predicted variations of the discharge rate with time based on the three models. Additionally, as before the *Phu* and *Psu* simulations consistently require less computational run time compared the $P\rho u$ model. Remarkably the effect is much more pronounced for the two-phase mixture (figure 8). The same observation was made in the case of the Isle of Grain pipeline containing a flashing liquid which undergoes two-phase transition upon depressurisation.

v) Despite the shorter pipeline employed, in all cases the computational run times for the two-phase pipeline are significantly greater than those for the pure liquid and permanent gas pipelines due to the flash calculations involved.

**Conclusion**

The numerical solutions for three different formulations of the conservation equations based on the dependent variables, *Phu*, *Psu* and the conventional $P\rho u$ for simulating the fluid dynamics following pipeline rupture were presented.

The above involved replacing the conservation equations with the corresponding characteristics and compatibility equations using MOC and solving them numerically at selected space and time intervals along the pipeline. The resulting positive and negative compatibility equations turned out to be identical for all of the three different formulations of the conservation equations. Only the path line compatibility was found to be different in each case.

Application of the three models to a the full bore rupture of a real pipeline containing a flashing liquid as well as relatively long hypothetical pipelines containing permanent gas, two-phase mixture and a pure liquid revealed significant differences in the computational

pipeline depending on the model used. For example in the case of the flashing liquid and two-phase mixture, the *Phu* and *Psu* based simulations required much lower computation rum time as opposed to the commonly employed $Pru$. In the case of the former, the fluid properties at the solution point may simply be obtained directly from *P/h* and *P/*s flash calculations. However, the determination of the fluid properties from the $Pru$ compatibility equation requires its iterative solution. The above becomes an extremely computationally expensive procedure especially for two-phase flows as numerous isothermal flash calculations are required in order to obtain an accurate solution.

The above is consistent with the observed relative insensitivity of the computational run with the choice of the dependent variables adopted in the simulation formulation for permanent gas and liquid pipelines as no flash calculations are involved.

Based on comparison with the Isle of Grain field data, the simulation results obtained using the *Phu* and *Psu* formulations were found to be more stable than those obtained using the $Pru$ formulation. The above was attributed to the less marked changes in the fluid entropy and enthalpy as compared to the fluid density when crossing the two-phase boundary.

In conclusion, using a fundamental approach, the present study addresses a major practical drawback associated with the long computational run times expended in simulating the fluid dynamics for highly transient flows such as those following the rupture of pressurised pipelines containing two-phase or flashing liquids. The significant reduction in the computational run time will be of considerable benefit to safety assessment engineers particularly in view of the rapid increase in the use of pressurised pipelines for the transport of hydrocarbons. A vast majority of these pipelines contain condensable gas or flashing liquid hydrocarbons that undergo two-phase transition upon rupture. Data on the subsequent fluid flow dynamics form the basis for all the major hazard consequence predictions associated with such type of failure including fire, explosion and environmental pollution.

Given the significant reductions in the computational run time afforded by the *Phu* based approach reported in this study, the technique has already been applied for the modelling of

outflow from pipeline networks (Mahgerefteh et. al, 2006a) and the study of low temperature induced fracture propagation in pressurised pipelines (Mahgerefteh et. al, 2006b).

**Acknowledgements**

The authors are grateful to the NATO Science programme for providing funding in support of this work.

**References**

Bond J, IChemE accidents database, IChemE, Rugby, UK (2002).

Bendiksen KH, Malnes D, Moe R, Nuland S. The dynamic two-fluid model OLGA: theory and applications, SPE Production Eng. 1991;6:171.

Bisgaard C, Sorensen HH, Spangenberg S. A finite element method for transient compressible flow in pipelines. Int. J. Num. Meth. Fluids. 1987;7: 291.

Chen JR, Richardson SM, Saville G. Numerical simulation of full-bore ruptures of pipelines containing perfect gases. Trans. Inst. Chem. Eng. Part B. 1992;70:59.

Chen JR, Richardson SM, Saville G. A simplified numerical method for transient two-phase pipe flow. Trans IChemE. 1993;71A:304.

Chen JR, Richardson SM, Saville G. Modelling of two-phase blowdown from pipelines – II. A simplified numerical method for multi-component mixtures. Chem. Eng. Sci. 1995; 50:2173.

Fairuzov YV. Blowdown of pipelines carrying flashing liquids. AIChE Journal. 1998; 44(5): 245.

Flatt R. Unsteady compressible flow in long pipelines following a rupture, Int. J. Num. Meth. Fluids. 1986; 6: 83.

Fletcher S. US senate ready to act on pipeline safety. Oil & Gas Journal. 2001;99.6:58.

Gato LMC, Henriques JCC. Dynamic behaviour of high-pressure natural-gas flow in pipelines. International Journal of Heat and Fluid Flow, 2005;26:817.

Georges A, Louvain-la-Neuve BE. Underground pipelines - The domino disaster of Ghislenghien, International Conference on Risk Perception, Communication, Acceptability; Technological Institute, Brugge, Belgium, 3-4 October 2005.

Lang E. Gas flow in pipelines following a rupture computed by a spectral method. J. Appl. Math. and Physics. 1991;42;183.

Lister M. The numerical solution of hyperbolic partial differential equations by the method of characteristics. Numerical methods for digital computers. New York: John Wiley and Sons, 1960.

Mahgerefteh H, Saha P, Economou IG. A study of the dynamic response of emergency shutdown valves following full-bore rupture of gas pipelines. Trans. Inst. Chem. Eng. Part B. 1997:75;201.

Mahgerefteh H, Saha P, Economou IG. Fast numerical simulation for full-bore rupture of pressurized pipelines. AIChE Journal. 1999; 45(6): 1191.

Mahgerefteh H, Saha P, Economou IG. Modelling fluid phase transition effects on dynamic behaviour of ESDV. AIChE Journal. 2000; 46(5):997.

Mahgerefteh H, Oke A, Atti, O. Modelling outflow following rupture in pipeline networks. Chem.Eng.Sci. 2006a; 61(6): 1811.

Mahgerefteh H, Atti, I. Modelling low temperature induced failure of pressurized pipelines. AIChEJ. 2006b; 52(3): 1248.

Myers GE. Analytical methods in conduction heat transfer. New York: McGraw-Hill, 1971.

Oke A, Mahgerefteh H, Economou IG, Rykov Y, A transient outflow model for pipeline puncture. Chem. Eng. Sci. 2003; 58(20): 4591.

Perry RH, Green DW. Perry's chemical engineers' handbook ($7^{th}$ edition). London: McGraw Hill, 1997.

Picard DJ, Bishnoi PR. The importance of real-fluid behaviour and non-isentropic effects in modelling compression characteristics of pipeline fluids for application in ductile fracture propagation analysis. Can. J. Chem. Eng. 1988;66:3.

Picard DJ, Bishnoi PR. The importance of real-fluid behaviour in predicting release rates resulting from high pressure sour-gas pipeline ruptures. Can. J. Chem. Eng. 1989; 67:3.

Prasad P, and Ravindran R, Partial differential equations, New Delhi: Wiley Eastern Limited, 1985.

Press WH, Teukolsky SA, Vetterling WT, Flannery BP. Numerical recipes in FORTRAN 77: The art of scientific computing (2nd edition). Cambridge: Cambridge University Press. 1994.

Richardson SM, Saville G, Isle of Grain pipeline depressurisation tests, HSE OTH 94441, HSE Books, HSE, Bootle, U.K. 1996a.

Richardson SM, Saville G, Blowdown of LPG pipelines, Trans. IChemE, 1996b:74B; 236.

Tiley CH. Pressure transient in a ruptured gas pipeline with friction and thermal effects included. PhD Thesis, City University, London, 1989.

U.S. Department of Transport, Code of Federation Regulations (CFR) Title 49D, Part 195, Transportation of hazardous liquids by pipeline. Accident Report Data Base.3 (1982 – 1997), 1997.

Versteeg HK, Malalasekera W. An introduction to computational fluid dynamics: the finite volume method. London: Prentice Hall. 1995.

Walas SM. Phase equilibrium in chemical engineering. Boston: Butterworth, 1987.

Wylie EB, Streeter VL. Fluid transients. New York: McGraw-Hill Inc., 1978.

Wylie EB, Streeter VL. Fluid transients in systems. New Jerse: Prentice- Hall, 1993.

Zucrow MJ, Hoffman JD. Gas dynamics (volumes I and II). New York: Wiley, 1976.

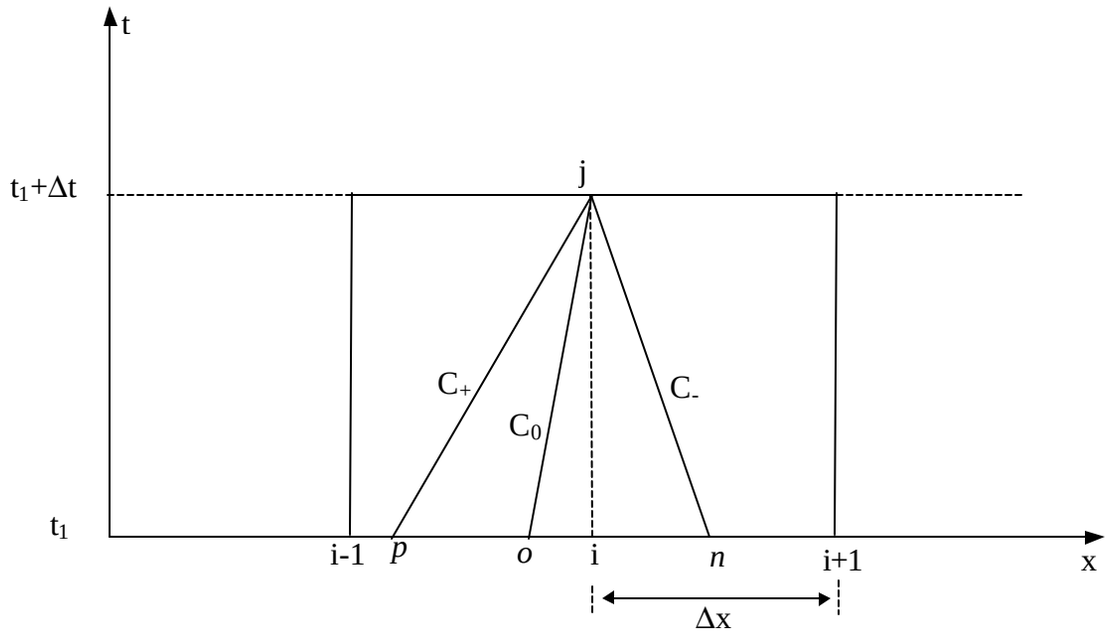


Figure 1: A schematic representation of Path line ($C_0$) and mach lines ($C_+$, $C_-$) characteristics at a grid point along the time (t) and space (x) axes.

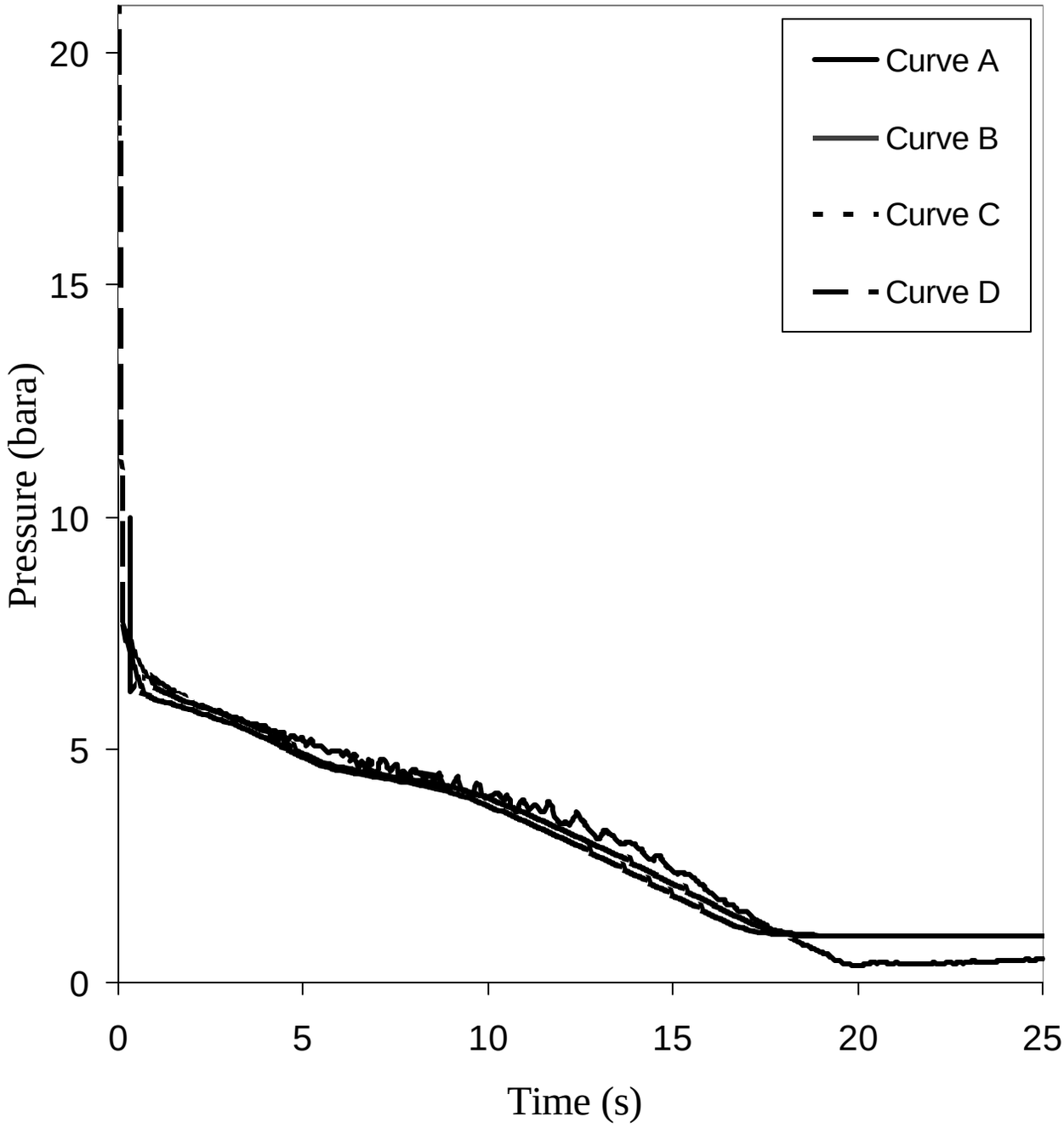


Figure 2: Experimental and simulated variations of the open end pressure with time following full bore rupture of the LPG pipeline.

Curve A: Measurement (Richardson and Saville, 1996a,b)
Curve B: Simulated data, $P\rho u$ model
Curve C: Simulated data, Phu model
Curve D: Simulated data, Psu model

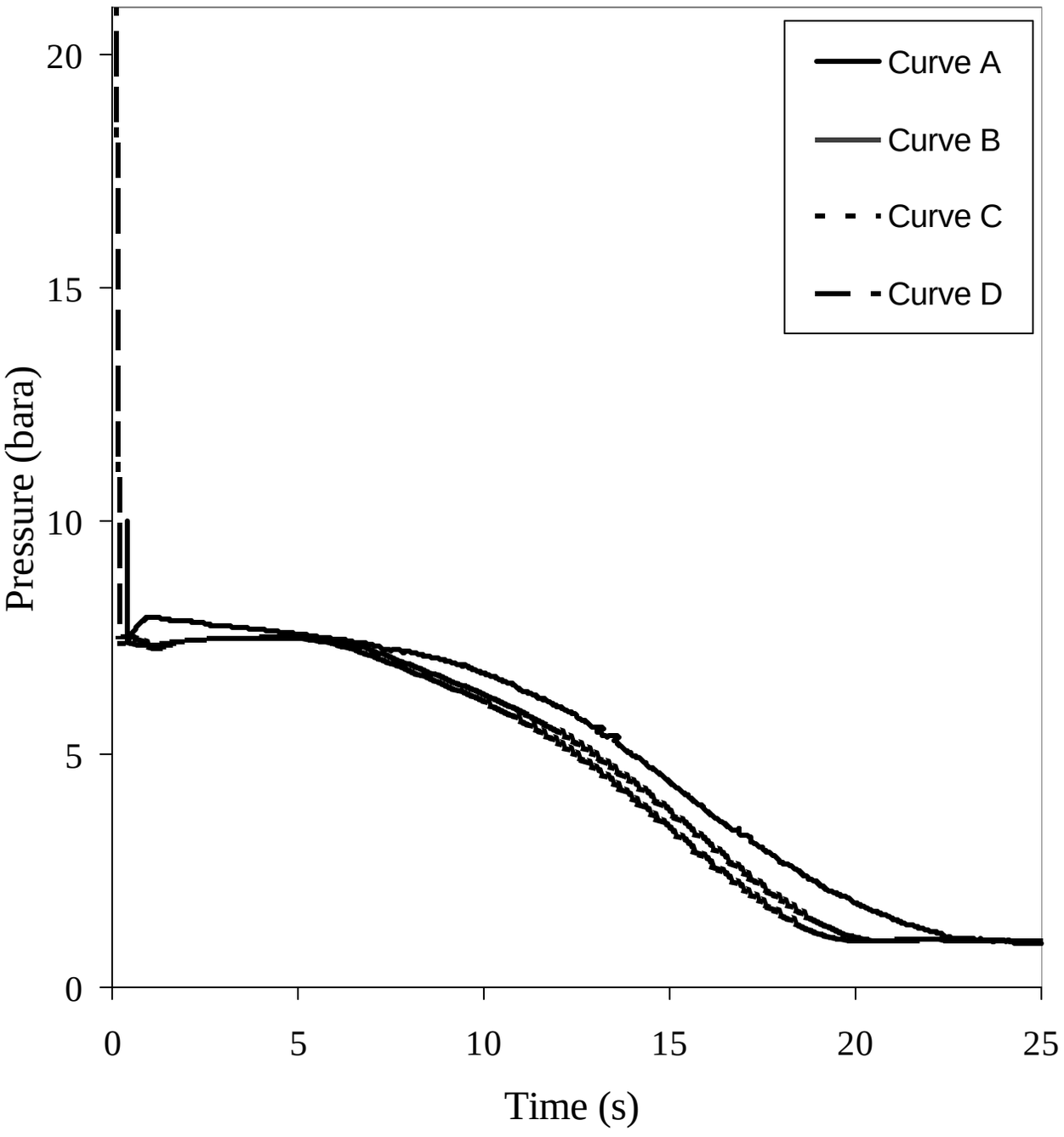


Figure 3: Experimental and simulated variations of the intact end pressure with time following full bore rupture of the LPG pipeline.

Curve A: Measurement (Richardson and Saville, 1996a,b)
Curve B: Simulated data, Pρu model
Curve C: Simulated data, Phu model
Curve D: Simulated data, Psu model

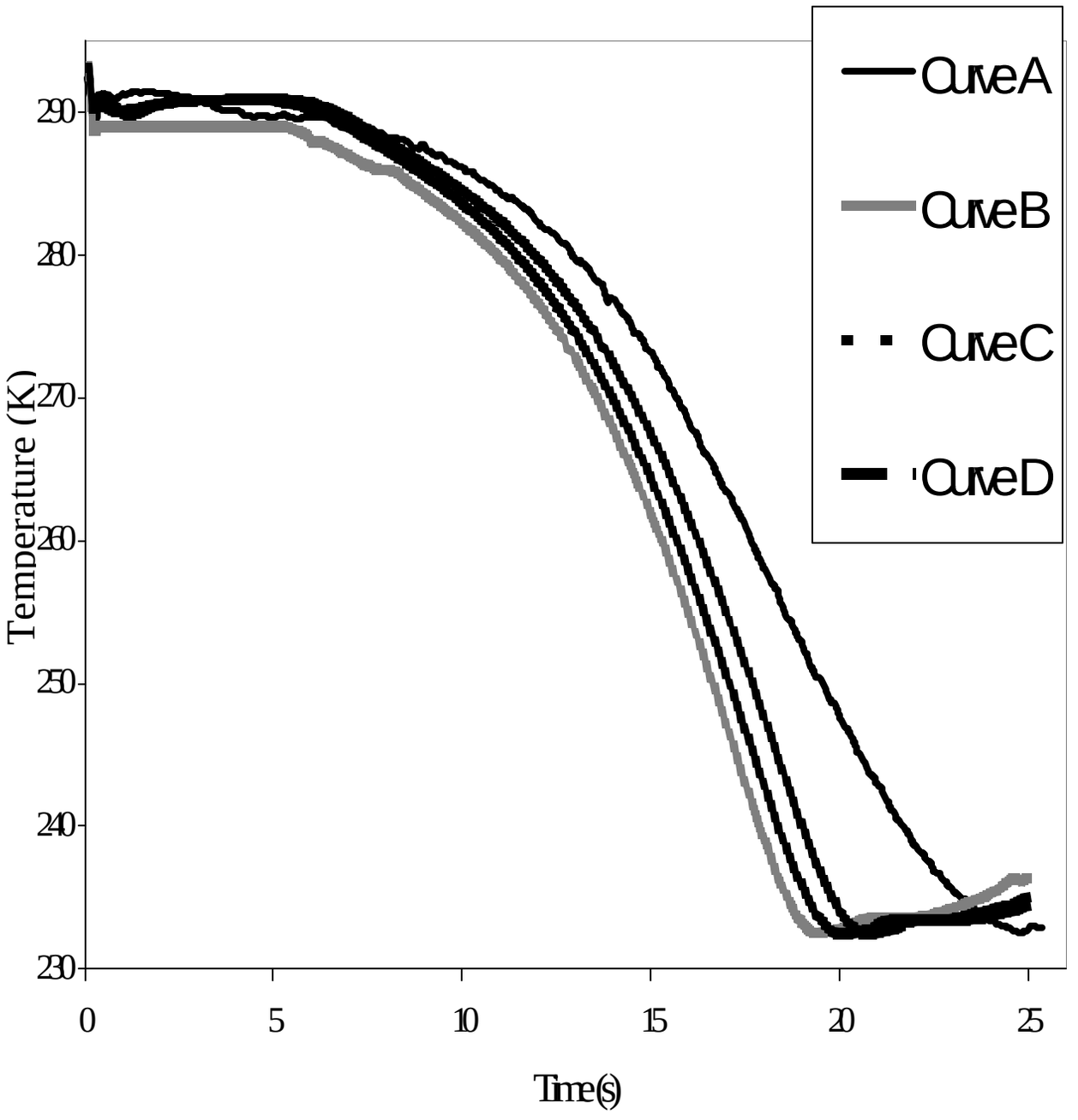


Figure 4: Experimental and simulated variations of the closed end temperature with time following full bore rupture of the LPG pipeline.

Curve A: Measurement (Richardson and Saville, 1996a,b)
Curve B: Simulated data, Ppu model

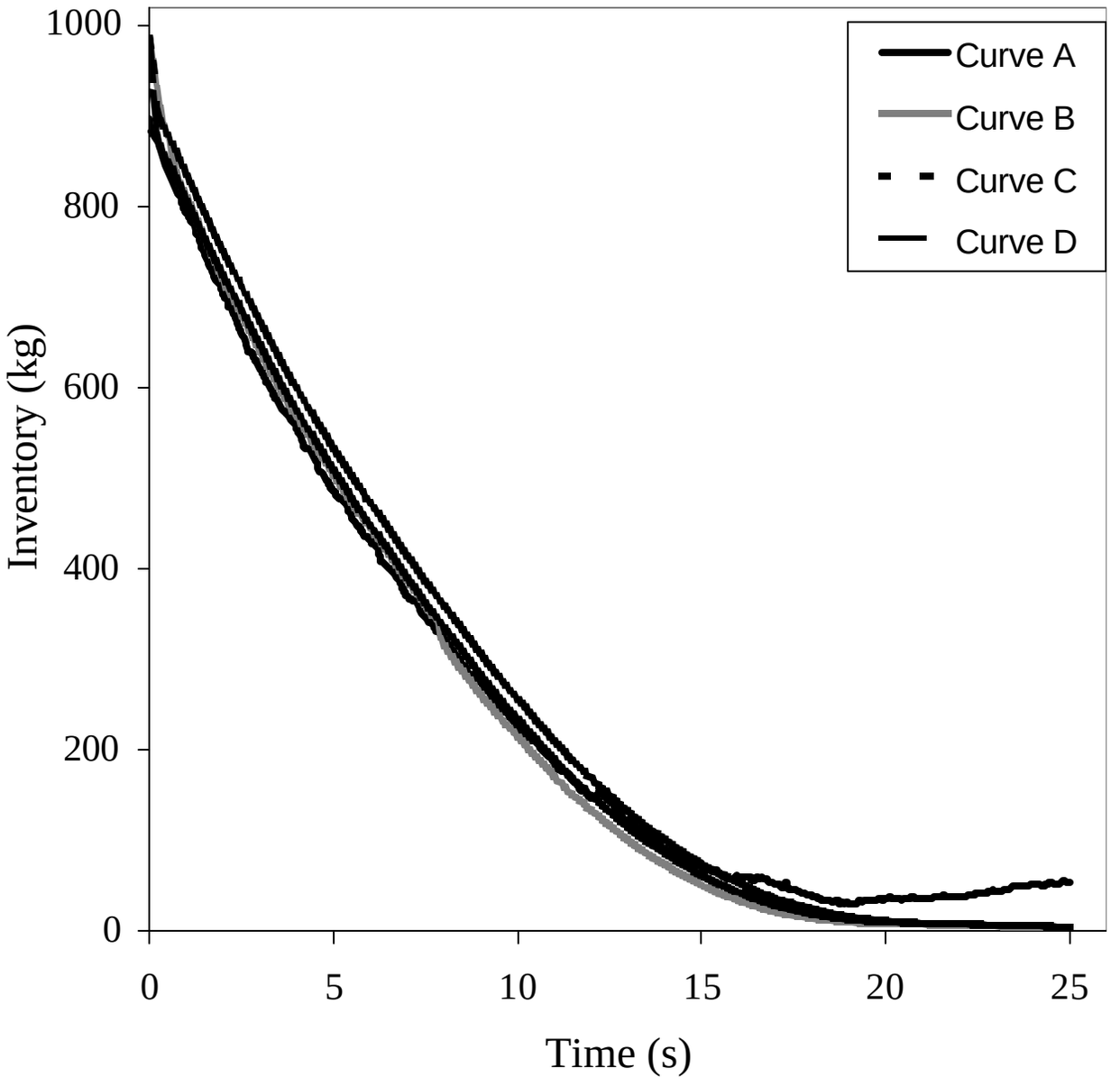


Figure 5: Experimental and simulated variations of the pipeline fluid inventory with time following full bore rupture of the LPG pipeline.

Curve A: Measurement (Richardson and Saville, 1996a,b)
Curve B: Simulated data, Pρu model
Curve C: Simulated data, Phu model
Curve D: Simulated data, Psu model

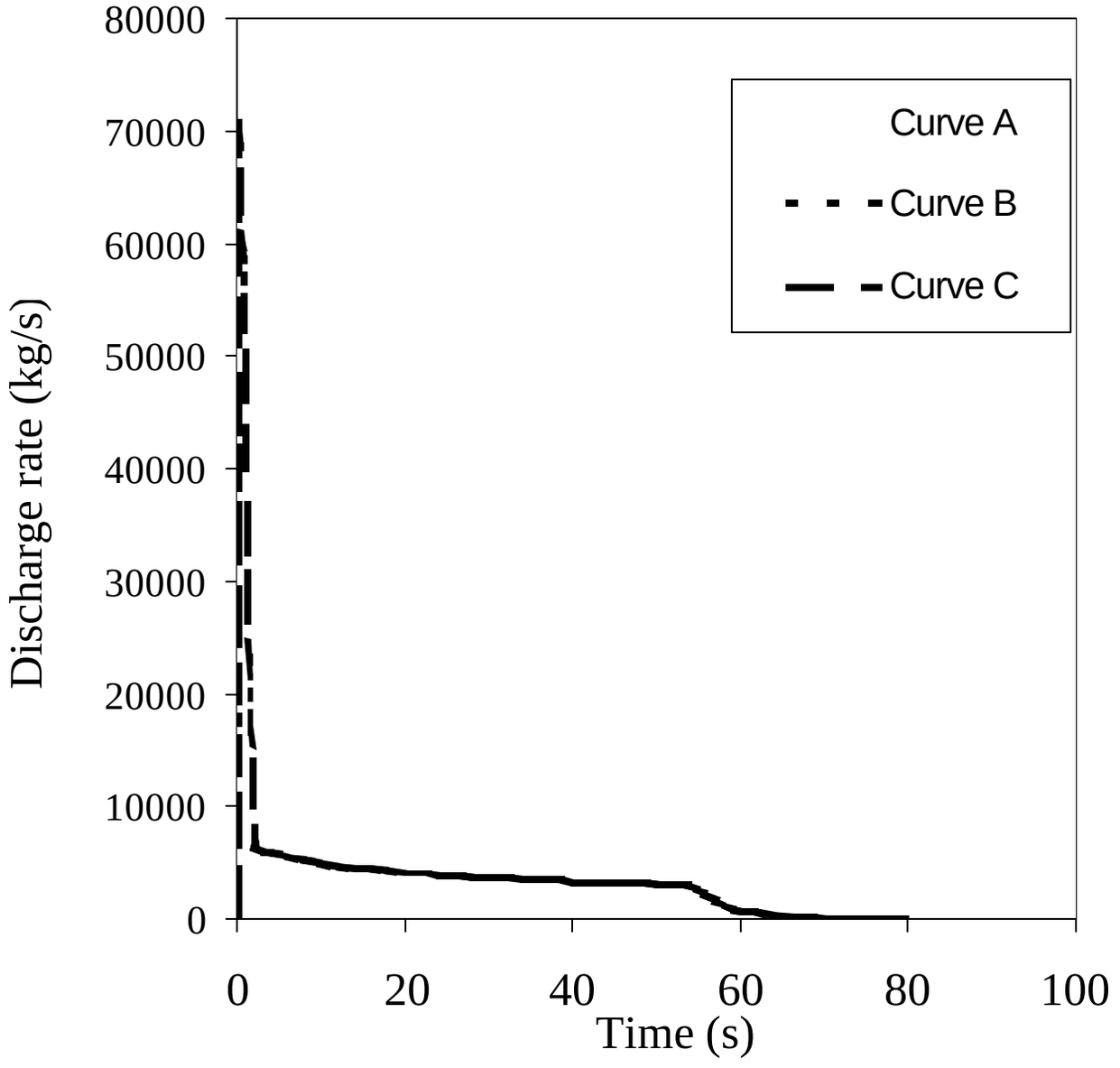


Figure 6. Simulated variation of discharge rate with time following full bore rupture for liquid pipeline (100% pentane) at 100 bara and 293.15 K.

Curve A: Pρu model; Computation run time, 1 hr 45 min
Curve B: Phu model; Computation run time: 1 hr 05 min
Curve C: Psu model; Computation run time: 1 hr 04 min

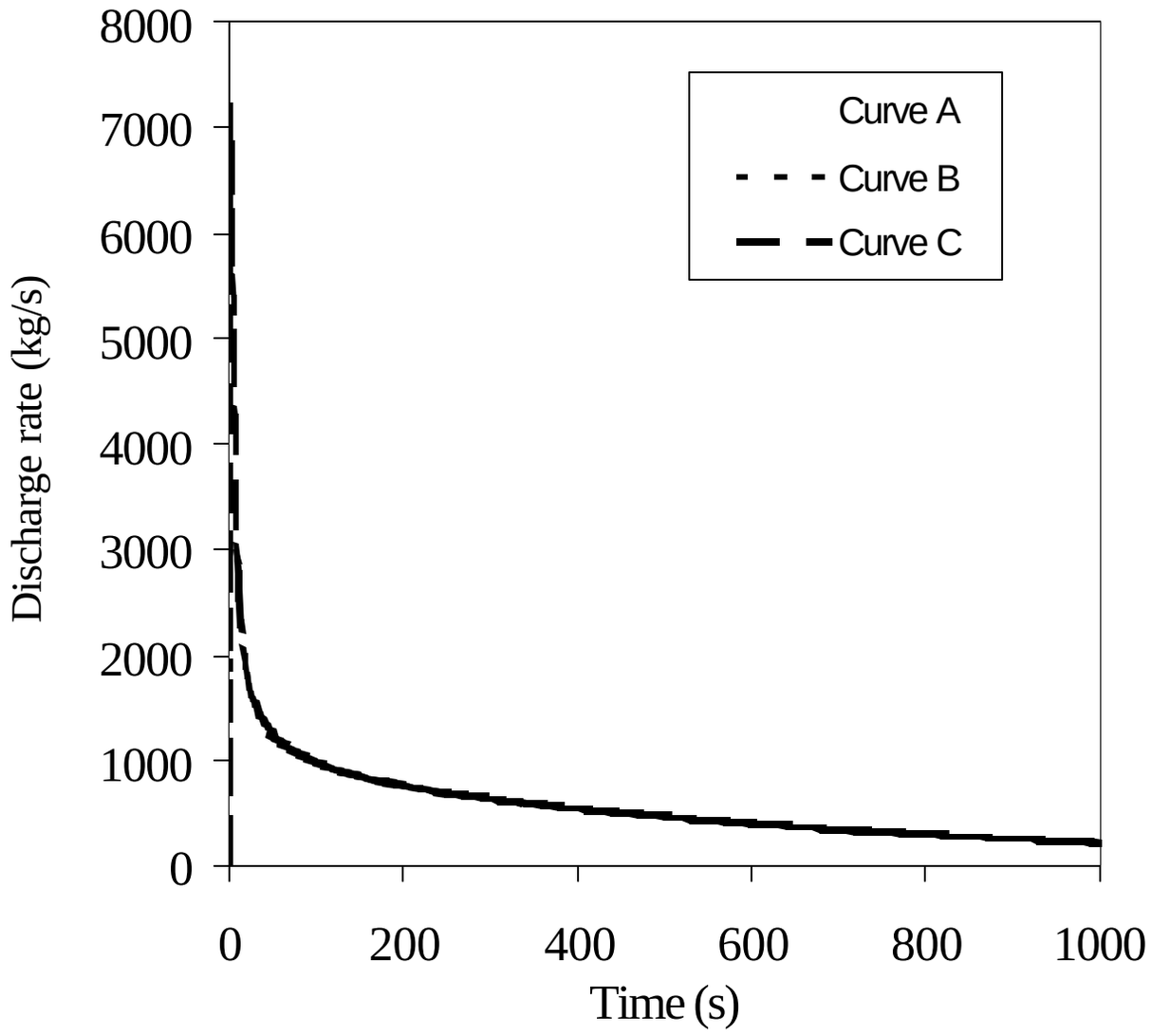


Figure 7. Simulated variation of discharge rate with time following full bore rupture for permanent gas pipeline (95% methane, 5% ethane) at 60 bara and 293.15 K.

Curve A: Pρu model; Computation run time: 1 hr 56 min
Curve B: Phu model; Computation run time: 1 hr 44 min
Curve C: Psu model; Computation run time: 1 hr 17 min

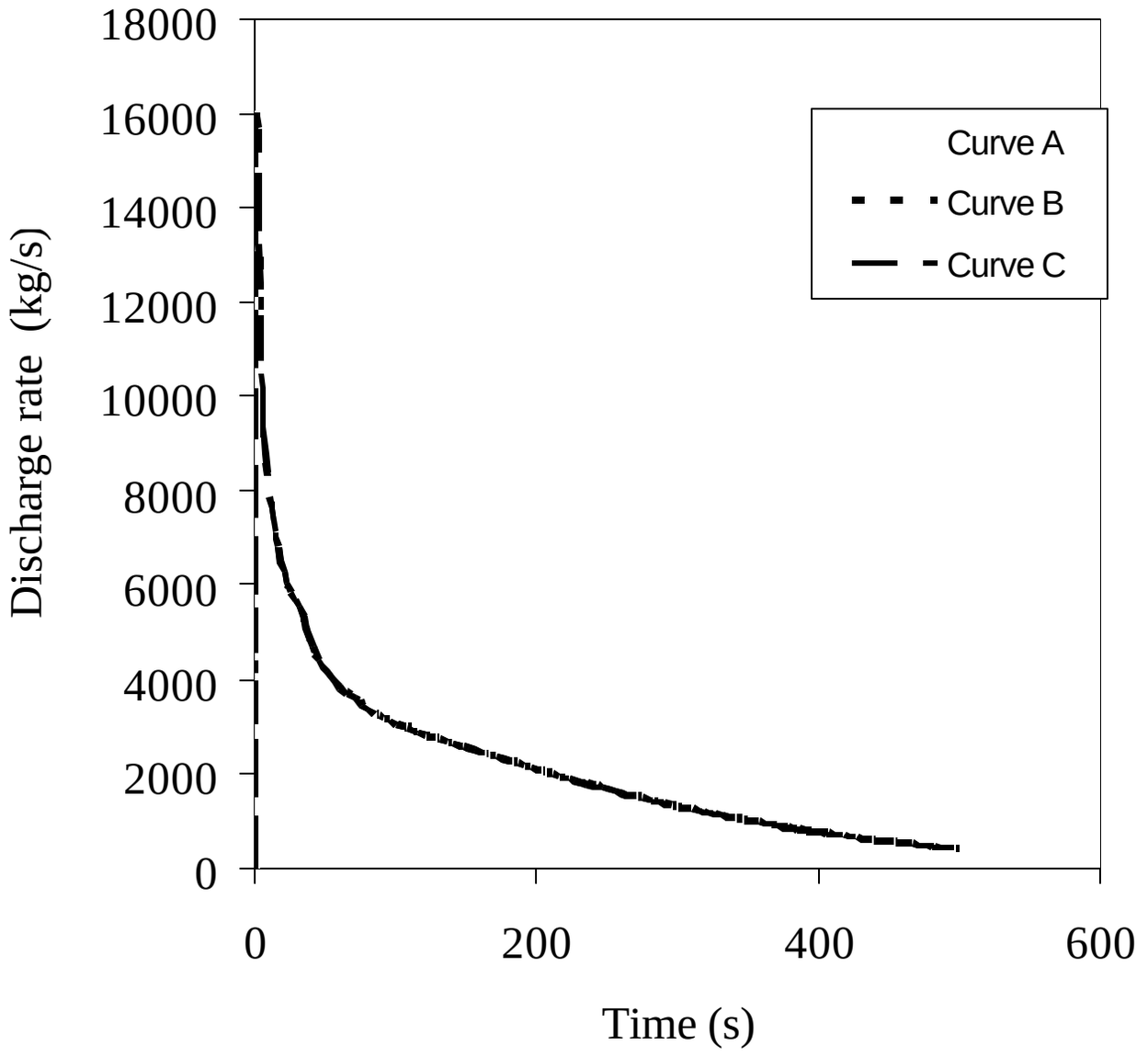


Figure 8 . Simulated variation of discharge rate with time following full bore rupture for two-phase (99% ethylene, 1% ethane) pipeline at 60 bara and 293.15 K.

Curve A: Pρu model; Computation run time: 43 hrs
Curve B: Phu model; Computation run time: 18 hrs
Curve C: Psu model; Computation run time: 24 hrs